

# The newly observed open-charm states in quark model

De-Min Li\*, Peng-Fei Ji, and Bing Ma,

Department of Physics, Zhengzhou University, Zhengzhou, Henan 450052, People's Republic of China

March 31, 2011

## Abstract

Comparing the measured properties of the newly observed open-charm states  $D(2550)$ ,  $D(2600)$ ,  $D(2750)$ ,  $D(2760)$ ,  $D_{s1}(2710)$ ,  $D_{sJ}(2860)$ , and  $D_{sJ}(3040)$  with our predicted spectroscopy and strong decays in a constituent quark model, we find that: (1) the  $D(2^1S_0)$  assignment to  $D(2550)$  remains open for its too broad width determined by experiment; (2) the  $D(2600)$  and  $D_{s1}(2710)$  can be identified as the  $2^3S_1$ - $1^3D_1$  mixtures; (3) if the  $D(2760)$  and  $D(2750)$  are indeed the same resonance, they would be the  $D(1^3D_3)$ ; otherwise, they could be assigned as the  $D(1^3D_3)$  and  $D'_2(1D)$ , respectively; (4) the  $D_{sJ}(2860)$  could be either the  $D_{s1}(2710)$ 's partner or the  $D_s(1^3D_3)$ ; and (5) both the  $D_{s1}(2P)$  and  $D'_{s1}(2P)$  interpretations for the  $D_{sJ}(3040)$  seem likely. The  $E1$  and  $M1$  radiative decays of these states are also studied. Further experimental efforts are needed to test the present quarkonium assignments for these new open-charm states.

**PACS numbers:** 12.39.-x, 13.20.Fc, 13.25.Ft, 14.40.Lb

---

\*lidm@zzu.edu.cn

## I. Introduction

In 2009, in inclusive  $e^+e^-$  interactions, two new charmed-strange states  $D_{s1}(2710)$  and  $D_{sJ}(2860)$  were observed by the BaBar Collaboration in both  $DK$  and  $D^*K$  channels[1]. The available experimental results on these two states are as follows:

$$M(D_{sJ}(2860)^+) = 2862 \pm 2^{+5}_{-2} \text{ MeV}, \Gamma(D_{sJ}(2860)^+) = 48 \pm 3 \pm 6 \text{ MeV}, \quad (1)$$

$$M(D_{s1}(2710)^+) = 2710 \pm 2^{+12}_{-7} \text{ MeV}, \Gamma(D_{s1}(2710)^+) = 149 \pm 7^{+39}_{-52} \text{ MeV}, \quad (2)$$

$$\frac{\mathcal{B}(D_{s1}(2710)^+ \rightarrow D^*K)}{\mathcal{B}(D_{s1}(2710)^+ \rightarrow DK)} = 0.91 \pm 0.13 \pm 0.12, \quad (3)$$

$$\frac{\mathcal{B}(D_{sJ}(2860)^+ \rightarrow D^*K)}{\mathcal{B}(D_{sJ}(2860)^+ \rightarrow DK)} = 1.10 \pm 0.15 \pm 0.19, \quad (4)$$

with  $DK = D^+K^0 + D^0K^+$  and  $D^*K = D^{*+}K^0 + D^{*0}K^+$ . In  $D^*K$  channel, the BaBar Collaboration also found the evidence for the  $D_{sJ}(3040)$  whose mass and width are  $3044 \pm 8^{+30}_{-5}$  MeV and  $239 \pm 35^{+46}_{-42}$  MeV, respectively. There is no signal of  $D_{sJ}(3040)$  in  $DK$  channel[1].

More recently, in inclusive  $e^+e^-$  collisions, four new charmed states  $D(2550)$ ,  $D(2600)$ ,  $D(2750)$ , and  $D(2760)$  were found by the BaBar Collaboration[2]. The  $D(2550)$  and  $D(2750)$  were observed in  $D^{*+}\pi^-$  channel, the  $D(2760)$  was observed in  $D^+\pi^-$  channel, and the  $D(2600)$  was observed in both  $D^{*+}\pi^-$  and  $D^+\pi^-$  channels. The isospin partners of the  $D(2600)^0$  and  $D(2760)^0$  were also observed in the  $D^0\pi^+$  channel. The resulting masses and widths of these four states with neutral-charge are

$$M(D(2550)^0) = 2539.4 \pm 4.5 \pm 6.8 \text{ MeV}, \Gamma(D(2550)^0) = 130 \pm 12 \pm 13 \text{ MeV}, \quad (5)$$

$$M(D(2600)^0) = 2608.7 \pm 2.4 \pm 2.5 \text{ MeV}, \Gamma(D(2600)^0) = 93 \pm 6 \pm 13 \text{ MeV}, \quad (6)$$

$$M(D(2760)^0) = 2763.3 \pm 2.3 \pm 2.3 \text{ MeV}, \Gamma(D(2760)^0) = 60.9 \pm 5.1 \pm 3.6 \text{ MeV}, \quad (7)$$

$$M(D(2750)^0) = 2752.4 \pm 1.7 \pm 2.7 \text{ MeV}, \Gamma(D(2750)^0) = 71 \pm 6 \pm 11 \text{ MeV}, \quad (8)$$

and the following ratios of branching fractions were also obtained :

$$\frac{\mathcal{B}(D(2600)^0 \rightarrow D^+\pi^-)}{\mathcal{B}(D(2600)^0 \rightarrow D^{*+}\pi^-)} = 0.32 \pm 0.02 \pm 0.09, \quad (9)$$

$$\frac{\mathcal{B}(D(2760)^0 \rightarrow D^+\pi^-)}{\mathcal{B}(D(2750)^0 \rightarrow D^{*+}\pi^-)} = 0.42 \pm 0.05 \pm 0.11. \quad (10)$$

Due to the poor information on the higher excitations of  $D$  and  $D_s$  mesons, the find of these open-charm states is clearly of importance to complete the  $D$  and  $D_s$  spectra. To understand

their observed properties, various efforts have been carried out under the assumption that all the observed open-charm states are dominated by the simple  $q\bar{q}$  quark content[3, 4, 5, 6, 3, 7, 8, 9, 10, 11, 12, 13, 14, 15, 16, 17]. It is natural and necessary to exhaust the possible conventional  $q\bar{q}$  descriptions before resorting to more exotic interpretations[18]. Further theoretical efforts are still required in order to satisfactorily explain the data concerning these open-charm states. In this work, we shall investigate the masses as well as strong and radiative decays of these newly observed states in the nonrelativistic constituent quark model and try to clarify their possible quarkonium assignments by comparing our predictions with the experiment.

The organization of this paper is as follows. In Sec. II, we calculate the open-charm mesons masses in a nonrelativistic constituent quark model and give the possible assignments for these open-charm states based on their observed masses and decay modes. In Sec. III, we investigate, with the  $^3P_0$  decay model, the strong decays of these states for different possible assignments. The radiative transitions of these states are given in Sec. IV. The summary and conclusion are given in Sec. V.

## II. Masses

To estimate the masses of  $c\bar{u}$  and  $c\bar{s}$  states, we employ a simple nonrelativistic constituent quark model which was proposed by Lakhina and Swanson and turns out to be able to describe the heavy-light meson and the charmonium masses with reasonable accuracy.[19]. In this model, the Hamiltonian is

$$H = H_0 + H_{sd} + C_{q\bar{q}}, \quad (11)$$

where  $H_0$  is the zeroth-order Hamiltonian,  $H_{sd}$  is the spin-dependent Hamiltonian, and  $C_{q\bar{q}}$  is a constant. The  $H_0$  is

$$H_0 = \frac{\mathbf{P}^2}{M_r} - \frac{4}{3} \frac{\alpha_s}{r} + br + \frac{32\alpha_s\sigma^3 e^{-\sigma^2 r^2}}{9\sqrt{\pi}m_q m_{\bar{q}}} \mathbf{S}_q \cdot \mathbf{S}_{\bar{q}}, \quad (12)$$

where  $r=|\mathbf{r}|$  is the  $q\bar{q}$  separation,  $M_r = 2m_q m_{\bar{q}}/(m_q + m_{\bar{q}})$ ;  $m_q$  and  $\mathbf{S}_q$  ( $m_{\bar{q}}$  and  $\mathbf{S}_{\bar{q}}$ ) are the mass and spin of the constituent quark  $q$  (antiquark  $\bar{q}$ ), respectively. The  $H_{sd}$  is

$$H_{sd} = \left( \frac{\mathbf{S}_q}{2m_q^2} + \frac{\mathbf{S}_{\bar{q}}}{2m_{\bar{q}}^2} \right) \cdot \mathbf{L} \left( \frac{1}{r} \frac{dV_c}{dr} + \frac{2}{r} \frac{dV_1}{dr} \right) + \frac{\mathbf{S}_+ \cdot \mathbf{L}}{m_q m_{\bar{q}}} \left( \frac{1}{r} \frac{dV_2}{dr} \right)$$

$$+ \frac{3\mathbf{S}_q \cdot \hat{\mathbf{r}}\mathbf{S}_{\bar{q}} \cdot \hat{\mathbf{r}} - \mathbf{S}_q \cdot \mathbf{S}_{\bar{q}}}{3m_q m_{\bar{q}}} V_3 + \left[ \left( \frac{\mathbf{S}_q}{m_q^2} - \frac{\mathbf{S}_{\bar{q}}}{m_{\bar{q}}^2} \right) + \frac{\mathbf{S}_-}{m_q m_{\bar{q}}} \right] \cdot \mathbf{L} V_4. \quad (13)$$

Here  $\mathbf{L}$  is the relative orbital angular momentum between  $q$  and  $\bar{q}$ , and

$$\begin{aligned} V_c &= -\frac{4}{3} \frac{\alpha_s}{r} + br, \\ V_1 &= -br - \frac{2}{9\pi} \frac{\alpha_s^2}{r} [9 \ln(\sqrt{m_q m_{\bar{q}}} r) + 9\gamma_E - 4], \\ V_2 &= -\frac{4}{3} \frac{\alpha_s}{r} - \frac{1}{9\pi} \frac{\alpha_s^2}{r} [-18 \ln(\sqrt{m_q m_{\bar{q}}} r) + 54 \ln(\mu r) + 36\gamma_E + 29], \\ V_3 &= \frac{4\alpha_s}{r^3} + \frac{1}{3\pi} \frac{\alpha_s^2}{r^3} [-36 \ln(\sqrt{m_q m_{\bar{q}}} r) + 54 \ln(\mu r) + 18\gamma_E + 31], \\ V_4 &= \frac{1}{\pi} \frac{\alpha_s^2}{r^3} \ln \left( \frac{m_{\bar{q}}}{m_q} \right), \\ \mathbf{S}_{\pm} &= \mathbf{S}_q \pm \mathbf{S}_{\bar{q}}, \end{aligned} \quad (14)$$

where  $\gamma_E = 0.5772$  and the scale  $\mu$  has been set to 1.3 GeV.

The model parameters have been chosen to reproduce the low lying  $D$  and  $D_s$  masses and are  $\alpha_s = 0.5$ ,  $b = 0.14$  GeV<sup>2</sup>,  $\sigma = 1.17$  GeV,  $C_{c\bar{u}} = -0.325$  GeV, and  $C_{c\bar{s}} = -0.275$  GeV. The constituent quark masses are taken to be  $m_c = 1.43$  GeV,  $m_u = m_d = 0.45$  GeV, and  $m_s = 0.55$  GeV. These quark masses are also used in both strong and radiative decays computations.

The heavy-light mesons are not the charge conjugation eigenstates and hence mixing can occur between the two states with  $J = L$ . This mixing can be parameterized as[20]

$$\begin{pmatrix} c\bar{q}(nL) \\ c\bar{q}'(nL) \end{pmatrix} = \begin{pmatrix} \cos \phi_L^{c\bar{q}} & \sin \phi_L^{c\bar{q}} \\ -\sin \phi_L^{c\bar{q}} & \cos \phi_L^{c\bar{q}} \end{pmatrix} \begin{pmatrix} n^1 L_L \\ n^3 L_L \end{pmatrix}, \quad (15)$$

where  $\phi$  is the mixing angle and  $q$  denotes  $u$  or  $s$  quark. The  $c\bar{q}'(nL)$  refers to the higher mass state.

With the help of the Mathematica program[21], solving the Schrödinger equation with Hamiltonian  $H_0$  and evaluating the  $H_{sd}$  in leading-order perturbation theory, one can obtain the open charm mesons masses as shown in Tables 1-2.<sup>1</sup> For comparison, the corresponding masses predicted by some other approaches such as the Blankenbecler-Sugar equation[22] and the relativistic quark model[20, 23, 24, 25] are also listed.

It is clear from Tables 1 and 2 that the quark model (11) can reasonably account for the masses of the observed ground  $S$  and  $P$ -wave open-charm mesons, and the overall agreement

---

<sup>1</sup>The mixing angles in radians are  $\phi_{1P}^{c\bar{u}} = 0.363$ ,  $\phi_{1P}^{c\bar{s}} = 0.427$ ,  $\phi_{2P}^{c\bar{u}} = 0.578$ ,  $\phi_{2P}^{c\bar{s}} = 0.564$ ,  $\phi_{1D}^{c\bar{u}} = 0.697$ ,  $\phi_{1D}^{c\bar{s}} = 0.701$ ,  $\phi_{2D}^{c\bar{u}} = 0.702$ , and  $\phi_{2D}^{c\bar{s}} = 0.708$ .

Table 1: The charmed meson masses in GeV.

State	$J^P$	This work	LNR[22]	ZVR[23]	EFG[24]	DE[25]	GI[20]	PDG[26]
$D(1^1S_0)$	$0^-$	1.867	1.874	1.85	1.871	1.868	1.88	1.869
$D(2^1S_0)$	$0^-$	2.555	2.540	2.50	2.581	2.589	2.58	
$D(1^3S_1)$	$1^-$	2.010	2.006	2.02	2.010	2.005	2.04	2.010
$D(2^3S_1)$	$1^-$	2.636	2.601	2.62	2.632	2.692	2.64	
$D(1^3P_0)$	$0^+$	2.252	2.341	2.27	2.406	2.377	2.40	2.308
$D(2^3P_0)$	$0^+$	2.752	2.758	2.78	2.919	2.949		
$D(1^3P_2)$	$2^+$	2.466	2.477	2.46	2.460	2.460	2.50	2.460
$D(2^3P_2)$	$2^+$	2.971	2.860	2.94	3.012	3.035		
$D_1(1P)$	$1^+$	2.402	2.389	2.40	2.426	2.417	2.44	2.427
$D'_1(1P)$	$1^+$	2.417	2.407	2.41	2.469	2.490	2.49	2.422
$D_1(2P)$	$1^+$	2.886	2.792	2.89	2.932	2.995		
$D'_1(2P)$	$1^+$	2.926	2.802	2.90	3.021	3.045		
$D(1^3D_1)$	$1^-$	2.740	2.750	2.71	2.788	2.795	2.82	
$D(2^3D_1)$	$1^-$	3.168	3.052	3.13	3.228			
$D(1^3D_3)$	$3^-$	2.719	2.688	2.78	2.863	2.799	2.83	
$D(2^3D_3)$	$3^-$	3.170	2.999	3.19	3.335			
$D_2(1D)$	$2^-$	2.693	2.689	2.74	2.806	2.775		
$D'_2(1D)$	$2^-$	2.789	2.727	2.76	2.850	2.833		
$D_2(2D)$	$2^-$	3.145	2.997	3.16	3.259			
$D'_2(2D)$	$2^-$	3.215	3.029	3.17	3.307			

between the expectations from the quark model (11) and those from other approaches, especially the Blankenbecler-Sugar equation[22] and the relativistic quark model[23], is good, which hence encourages us to discuss the possible assignments for the newly observed open-charm states based on the expectations of our employed quark model. Among these newly observed open-charm states, the  $J^P$  of  $D_{s1}(2710)$  is determined to be  $1^-$  experimentally[27], while the spin-parity quantum numbers of the other states are still unsettled. According to the observed decay modes, the possible spin-parity quantum numbers of these open-charm states are listed in Table 3.

We shall discuss the possible quarkonium assignments for these open-charm states based on Tables 1, 2 and 3. The possible  $J^P$  of  $D(2550)$  are  $0^-$ ,  $1^-$ ,  $2^-$ ,  $\dots$ . The  $1^-[D(2^3S_1, 1^3D_1)]$  and  $2^-[D^{(\prime)}_{s2}(2D)]$  are expected to be at least about 100 MeV higher than  $D(2550)$  in mass. the  $1^-$  and  $2^-$  assignments to  $D(2550)$  are implausible. The  $D(2550)$  mass is very close to the predicted mass for the  $0^-[D(2^1S_0)](2555 \text{ MeV})$  and the helicity-angle distribution of  $D(2550)$

Table 2: The charm-strange meson masses in GeV.

State	$J^P$	This work	LNR[22]	ZVR[23]	EFG[24]	DE[25]	GI[20]	PDG[26]
$D_s(1^1S_0)$	$0^-$	1.969	1.975	1.94	1.969	1.965	1.98	1.969
$D_s(2^1S_0)$	$0^-$	2.640	2.659	2.61	2.688	2.700	2.67	
$D_s(1^3S_1)$	$1^-$	2.107	2.108	2.13	2.111	2.113	2.13	2.112
$D_s(2^3S_1)$	$1^-$	2.714	2.722	2.73	2.731	2.806	2.73	
$D_s(1^3P_0)$	$0^+$	2.344	2.455	2.38	2.509	2.487	2.48	2.317
$D_s(2^3P_0)$	$0^+$	2.830	2.901	2.90	3.054	3.067		
$D_s(1^3P_2)$	$2^+$	2.559	2.586	2.58	2.571	2.581	2.59	2.572
$D_s(2^3P_2)$	$2^+$	3.040	2.988	3.06	3.142	3.157		
$D_{s1}(1P)$	$1^+$	2.488	2.502	2.51	2.536	2.535	2.53	2.459
$D'_{s1}(1P)$	$1^+$	2.510	2.522	2.52	2.574	2.605	2.57	2.535
$D_{s1}(2P)$	$1^+$	2.958	2.928	3.00	3.067	3.114		
$D'_{s1}(2P)$	$1^+$	2.995	2.942	3.01	3.154	3.165		
$D_s(1^3D_1)$	$1^-$	2.804	2.845	2.82	2.913	2.913	2.90	
$D_s(2^3D_1)$	$1^-$	3.217	3.172	3.25	3.383			
$D_s(1^3D_3)$	$3^-$	2.811	2.844	2.90	2.917	2.925	2.92	
$D_s(2^3D_3)$	$3^-$	3.240	3.157	3.31	3.469			
$D_{s2}(1D)$	$2^-$	2.788	2.817	2.86	2.931	2.900		
$D'_{s2}(1D)$	$2^-$	2.849	2.844	2.88	2.961	2.953		
$D_{s2}(2D)$	$2^-$	3.217	3.144	3.28	3.403			
$D'_{s2}(2D)$	$2^-$	3.260	3.167	3.29	3.456			

turns out to be consistent with the predictions for  $D(2^1S_0)$ [2]. Therefore, the  $0^-[D(2^1S_0)]$  assignment to  $D(2550)$  seems the most plausible. The possible  $J^P$  of  $D(2600)$  are  $1^-$ ,  $3^-$ ,  $\dots$ . The  $D(2600)$  mass is very close to the predicted mass for the  $1^-[D(2^3S_1)]$  (2636 MeV). Also, the  $D(2^3S_1)$  and  $D(1^3D_1)$  have the same  $J^P$  and similar masses, and hence in general can mix to produce two physical  $1^-$  states<sup>2</sup>. Therefore, the  $D(2600)$  is most likely the  $2^3S_1$ - $1^3D_1$  mixtures  $1^-[D(2S$ - $1D)]$ . The helicity-angle distribution of  $D(2600)$  is found to be also consistent with the

<sup>2</sup>Hereafter, we shall assign the  $1^-$  physical states as the  $2^3S_1$ - $1^3D_1$  mixtures.

Table 3: Possible  $J^P$  of the open-charm states based on the observed decay modes.

State	observed channel	Possible $J^P$
$D(2550)$	$D^*\pi$	$0^-, 1^-, 2^-\dots$
$D(2600)$	$D\pi, D^*\pi$	$1^-, 3^-\dots$
$D(2750)$	$D^*\pi$	$0^-, 1^-, 2^-, 3^-\dots$
$D(2760)$	$D\pi$	$0^+, 1^-, 2^+, 3^-\dots$
$D_{sJ}(2860)$	$DK, D^*K$	$1^-, 3^-\dots$
$D_{sJ}(3040)$	$D^*K$	$0^-, 1^+, 2^-\dots$

predicted  $D(2^3S_1)$  or  $D(1^3D_1)$ [2]. Similarly, the  $D_{s1}(2710)$  is most likely the  $1^-[D_s(2S-1D)]$ . The possible  $J^P$  of  $D(2750)$  include  $0^-, 1^-, 2^-, 3^-, \dots$ . The  $D(2750)$  mass is about 200 MeV higher than that of  $0^-[D(2^1S_0)]$ , which makes the  $0^-$  assignment to  $D(2750)$  implausible. The  $D(2750)$  mass is very close to the masses of  $1^-[D(1^3D_1)](2740 \text{ MeV})$ ,  $3^-[D(1^3D_3)](2719 \text{ MeV})$ ,  $2^-[D_2(1D)](2693 \text{ MeV})$ , and  $2^-[D'_2(1D)](2789 \text{ MeV})$ . Therefore, the plausible assignments for  $D(2750)$  would be  $1^-[D(2S-1D)]$ ,  $3^-[D(1^3D_3)]$ , and  $2^-[D_2(1D), D'_2(1D)]$ . The possible  $J^P$  of  $D(2760)$  include  $0^+, 1^-, 2^+, 3^-, \dots$ . The mass difference between the  $D(2760)$  and  $2^+[D(1^3P_2, 2^3P_2)]$  is about 200 MeV while the  $D(2750)$  mass is very close to the masses of  $1^-[D(1^3D_1)](2740 \text{ MeV})$ ,  $3^-[D(1^3D_3)](2719 \text{ MeV})$ , and  $0^+[D(2^3P_0)](2752 \text{ MeV})$ , which makes  $1^-[D(2S-1D)]$ ,  $3^-D(1^3D_3)$ , and  $0^+D(2^3P_0)]$  assignments to  $D(2760)$  possible. The possible  $J^P$  of the  $D_{sJ}(2860)$  are  $1^-, 3^-, \dots$ . Since the  $D_{sJ}(2860)$  mass is close to  $1^-[D_s(1^3D_1)]$  mass (2804 MeV) and  $3^-[D_s(1^3D_3)]$  mass (2811 MeV), the possible assignments for  $D_{sJ}(2860)$  include  $1^-[D_s(2S-1D)]$  and  $3^-[D_s(1^3D_3)]$ . The possible  $J^P$  of  $D_{sJ}(3040)$  are  $0^-, 1^+, 2^-, \dots$ . The  $D_{sJ}(3040)$  is far higher than the  $0^-[D_s(2^3S_1)]$  and  $2^-[D_{s2}^{(\prime)}(1D)]$  in mass. Also, the  $2^-[D_{s2}^{(\prime)}(2D)]$  mass is about 200 MeV higher than that of  $D_{sJ}(3040)$ . The possibility of  $D_{sJ}(3040)$  being the  $0^-$  and  $2^-$  can be ruled out. The  $D_{sJ}(3040)$  mass is close to the quark model expectations for the  $1^+[D_{s1}^{(\prime)}(1P)]$  mass, therefore the  $1^+[D_{s1}^{(\prime)}(1P)]$  assignment to  $D_{sJ}(3040)$  becomes the most possible.

Below, we shall focus on these possible assignments for the observed open-charm states as shown in Table 4. The mass information alone is insufficient to classify these new open-charm states. Their decay properties also need to be compared with model expectations. We shall discuss the decay dynamics of these states in next section.

### III. Strong decays

#### A. Model parameters

In this section, we shall employ the  $^3P_0$  model to evaluate the tow-body open-flavor strong decays of the initial state. The  $^3P_0$  model, also known as the quark pair creation model, has been extensively applied to evaluate the strong decays of mesons from light  $q\bar{q}$  to heavy  $c\bar{b}$ , since

Table 4: Possible assignments of the open-charm states based on their masses and decay modes.

State	Assignments
$D(2550)$	$0^- [D(2^1S_0)]$
$D(2600)$	$1^- [D(2S-1D)]$
$D(2750)$	$1^- [D(2S-1D)], 2^- [D_2(1D), D'_2(1D)], 3^- [D(1^3D_3)]$
$D(2760)$	$1^- [D(2S-1D)], 3^- [D(1^3D_3)], 0^+ [D(2^3P_0)]$
$D_{s1}(2710)$	$1^- [D_s(2S-1D)]$
$D_{sJ}(2860)$	$1^- [D_s(2S-1D)], 3^- [D_s(1^3D_3)]$
$D_{sJ}(3040)$	$1^+ [D_{s1}(2P), D'_{s1}(2P)]$

it gives a considerably good description of many observed decay amplitudes and partial widths of hadrons. Some detailed reviews on the  $^3P_0$  model can be found in Refs.[28, 29, 30, 31, 32]. Also, the simple harmonic oscillator (SHO) approximation for spatial wave functions of mesons is used in the strong decays computations. This is typical of strong decay calculations. The SHO wave functions have the advantage that decay amplitudes and widths can be determined analytically, and it has been demonstrated that the numerical results are usually not strongly dependent on the details of the spatial wave functions of mesons[32, 33, 34, 35]. The explicit expression for the decay width employed in this work can be seen in Refs.[36].

The parameters involved in the  $^3P_0$  model include the constituent quarks masses, the SHO wave function scale parameters  $\beta$ 's, and the light nonstrange quark pair creation strength  $\gamma$ . The  $\gamma$  and the strange quark pair creation strength  $\gamma_{s\bar{s}}$  can be related by  $\gamma_{s\bar{s}} \approx \gamma/\sqrt{3}$ [37]. The constituent quarks masses  $m_u$ ,  $m_d$ ,  $m_s$ , and  $m_c$  are the same as those used in the constituent quark model (11). The SHO wave function scale parameters are taken to be the effective  $\beta$ 's obtained by equating the root mean square radius of the SHO wave function to that obtained from the nonrelativistic quark model (11). The meson effective  $\beta$ 's used in this work are listed in Table 5. The remaining parameter  $\gamma$  is an overall factor in the width. By fitting to 19 well-established experimental decay widths,<sup>3</sup> we obtain  $\gamma = 0.452 \pm 0.105$ , consistent with  $0.485 \pm 0.15$  obtained by Close and Swanson from their model[38]. The  $\gamma$  uncertainty means that the

<sup>3</sup>The decay modes used in our fit are [1]  $\rho \rightarrow \pi\pi$ , [2]  $\phi \rightarrow KK$ , [3]  $K^* \rightarrow K\pi$ , [4]  $b_1 \rightarrow \omega\pi$ , [5]  $K_2^* \rightarrow K\pi$ , [6]  $K_2^* \rightarrow K^*\pi$ , [7]  $K_2^* \rightarrow K\rho$ , [8]  $K_2^* \rightarrow K\omega$ , [9]  $\pi_2(1670) \rightarrow f_2\pi$ , [10]  $\pi_2(1670) \rightarrow K^*K$ , [11]  $\rho_3(1680) \rightarrow \pi\pi$ , [12]  $\rho_3(1680) \rightarrow \omega\pi$ , [13]  $\rho_3(1680) \rightarrow KK$ , [14]  $K_3(1780) \rightarrow K\pi$ , [15]  $K_3(1780) \rightarrow K\rho$ , [16]  $K_3(1780) \rightarrow K^*\pi$ , [17]  $D_2(2460)^0 \rightarrow D\pi + D^*\pi$ , [18]  $D_2(2460)^+ \rightarrow D\pi + D^*\pi$ , and [19]  $D_{s2} \rightarrow DK + D^*K + D_s\eta$ . The corresponding data are from PDG[26].



theoretical width has an uncertainty of  $\delta\Gamma \simeq 0.47\Gamma$ . It is perhaps no surprise that the prediction has a larger uncertainty due to the larger errors of data as well as the decay model which is tuned for strong decays of momenta of hundreds of MeV.

The meson masses used to determine the phase space and final state momenta in both strong and radiative decays computations are [1, 2, 26]  $M_{\pi^\pm} = 139.57$  MeV,  $M_{\pi^0} = 134.98$  MeV,  $M_{K^\pm} = 493.677$  MeV,  $M_{K^0} = 497.614$  MeV,  $M_\eta = 547.853$  MeV,  $M_\rho = 775.49$  MeV,  $M_\omega = 782.65$  MeV,  $M_{K^{*\pm}} = 891.66$  MeV,  $M_{K^{*0}} = 896$  MeV,  $M_{D^\pm} = 1869.62$  MeV,  $M_{D^0} = 1864.84$  MeV,  $M_{D^{*\pm}} = 2010.27$  MeV,  $M_{D^{*0}} = 2006.97$  MeV,  $M_{D_s} = 1968.49$  MeV,  $M_{D_s^*} = 2112.3$  MeV,  $M_{D_1(2430)^0} = M_{D_1(2430)^\pm} = 2427$  MeV,  $M_{D_1(2420)^\pm} = 2423.4$  MeV,  $M_{D_1(2420)^0} = 2422.3$  MeV,  $M_{D_0(2400)^0} = 2308$  MeV,  $M_{D_0(2400)^\pm} = 2403$  MeV,  $M_{D_2(2460)^\pm} = 2460.1$  MeV,  $M_{D_2(2460)^0} = 2461.1$  MeV,  $M_{D_{s1}(2460)} = 2459.6$  MeV,  $M_{D_{s1}(2535)} = 2535.35$  MeV,  $M_{D_{s0}(2317)} = 2317.8$  MeV,  $M_{D_{s2}(2573)} = 2572.6$  MeV,  $M_{D(2550)^0} = 2539.4$  MeV,  $M_{D(2600)^0} = 2608.7$  MeV,  $M_{D(2760)^0} = 2763.3$  MeV,  $M_{D(2750)^0} = 2752.4$  MeV,  $M_{D_{s1}(2710)} = 2710$  MeV,  $M_{D_{sJ}(2860)} = 2862$  MeV, and  $M_{D_{sJ}(3040)} = 3044$  MeV. The meson flavor functions follow the conventions of Ref.[20], for example,  $D^0 = c\bar{u}$ ,  $D^+ = -c\bar{d}$ ,  $D_s^+ = -c\bar{s}$ ,  $K^+ = -u\bar{s}$ ,  $K^- = s\bar{u}$ ,  $K^0 = -d\bar{s}$ ,  $\pi^+ = -u\bar{d}$ ,  $\pi^0 = (u\bar{u} - d\bar{d})/\sqrt{2}$ ,  $\phi = -s\bar{s}$ ,  $\omega = (u\bar{u} + d\bar{d})/\sqrt{2}$ , and  $\eta = (u\bar{u} + d\bar{d})/2 - s\bar{s}/\sqrt{2}$ . Also, we set  $D_1(1P) = D_1(2430)$ ,  $D'_1(1P) = D_1(2420)$ ,  $D_{s1}(1P) = D_{s1}(2460)$ , and  $D'_{s1}(1P) = D_{s1}(2535)$ . The  $n^3L_J$ - $n^1L_J$  mixing angles are taken as those determined in the mass estimates.

Table 5: The meson effective  $\beta$  values in MeV.

$n^{2S+1}L_J$	$u\bar{u}$	$u\bar{s}$	$s\bar{s}$	$c\bar{u}$	$c\bar{s}$
$1^1S_0$	470	466	470	453	484
$2^1S_0$	294	301	310	325	343
$1^3S_1$	308	322	338	379	406
$2^3S_1$	258	267	279	306	324
$1^3P_J$	280	290	302	328	348
$2^3P_J$	247	255	265	287	303
$1^1P_1$	284	294	306	332	352
$2^1P_1$	250	259	269	290	306
$1^3D_J$	261	270	281	304	321
$2^3D_J$	238	246	255	275	290
$1^1D_2$	261	270	281	304	321
$2^1D_2$	238	246	255	275	290

## B. $D(2550)$

The decay widths of  $D(2550)$  as  $D(2^1S_0)$  are shown in Table 6. The predicted total width is about 45 MeV, about 70 MeV lower than the lower limit of the measured  $\Gamma(D(2550)) = 130 \pm 12 \pm 13$  MeV. The recent calculations in a  $^3P_0$  model[15] and a chiral quark model[16] also give a rather narrow width for the  $D(2^1S_0)$ . The upper limit of the  $D(2^1S_0)$ 's width is expected to be about 66 MeV, still about 50 MeV lower than the lower limit of the measurement. This inconsistency between the theoretical and experimental results could imply that the experimental analysis has overestimated the width of  $D(2550)$  if this state is indeed the  $2^1S_0$  charmed meson, as suggested by Ref.[15]. Further confirmation of its resonance parameters is required to confirm the  $D(2^1S_0)$  assignment to  $D(2550)$ . The ratio  $\Gamma(D_0(2400)\pi)/\Gamma(D^*\pi)$  is expected to be about 0.22, which is independent of the parameter  $\gamma$  and can also present a consistent check for this assignment. Without additional information on  $D(2550)$ , the  $D(2^1S_0)$  assignment to  $D(2550)$  would remain open.

Table 6: Decay widths of  $D(2550)$  as  $D(2^1S_0)$  in MeV.

$D^{*+}\pi^-$	$D^{*0}\pi^0$	$D_0(2400)^0\pi^0$	Total
24.86	12.41	8.09	45.35

## C. $D(2600)$

In the 2S-1D mixing scenario, the eigenvectors of  $D_1(2600)$  and its partner  $D_1(M_X)$  can be written as

$$|D(2600)\rangle = \cos\theta|2^3S_1\rangle - \sin\theta|1^3D_1\rangle, \quad (16)$$

$$|D(M_X)\rangle = \sin\theta|2^3S_1\rangle + \cos\theta|1^3D_1\rangle, \quad (17)$$

where the  $\theta$  is the  $D(2^3S_1)$ - $D(1^3D_1)$  mixing angle and  $M_X$  denotes the mass of the physical state  $D_1(M_X)$ .

The predicted decay widths of  $D(2600)$  are listed in Table 7. The variations of decay widths and branching ratio  $\Gamma(D^+\pi)/\Gamma(D^{*+}\pi^-)$  with the mixing angle  $\theta$  are illustrated in Fig. 1. It is clear that in the presence of about  $0.364 \leq \theta \leq 0.4$  radians, both the total width and branching

ratio  $\Gamma(D^+\pi)/\Gamma(D^{*+}\pi^-)$  of  $D(2600)$  can be well reproduced (see Fig. 1(a)). Also in this mixing angle range, the  $D^*\pi$ ,  $D_1(2420)\pi$ , and  $D\pi$  are the dominant decay modes and the mode  $D^{*+}\pi^-$  dominates  $D^+\pi^-$  (see Fig. 1(b)), consistent with the observation. The helicity-angle distribution of  $D(2600)$  is also found to be consistent with the predictions for the  $D(2^3S_1)$  or  $D(1^3D_1)$ [2]. Therefore the interpretation of  $D(2600)$  as a mixture of the  $D(2^3S_1)$  and  $D(1^3D_1)$  seems convincing. It is expected that  $\Gamma(D_1(2420)\pi)/\Gamma(D^*\pi)$  is around 1.0 and  $\Gamma(D_1(2430)\pi)/\Gamma(D^*\eta)$  is  $1.1 \sim 1.4$ . Further experimental study on the  $D(2600)$  in the  $D_1(2420)\pi$ ,  $D_1(2430)\pi$ , and  $D^*\eta$  channels can present a consistent check for this interpretation.

Table 7: Decay widths of  $D(2600)$  as the  $1^-$  state in MeV.  $c \equiv \cos\theta$  and  $s \equiv \sin\theta$ .

Mode	$\Gamma_i$
$D^0\pi^0$	$0.02c^2 + 1.28cs + 25.90s^2$
$D^+\pi^-$	$0.02c^2 + 1.77cs + 51.89s^2$
$D_s K$	$0.32c^2 - 3.17cs + 7.86s^2$
$D\eta$	$0.50c^2 - 4.70cs + 10.99s^2$
$D^{*0}\pi^0$	$3.62c^2 + 13.42cs + 12.45s^2$
$D^{*+}\pi^-$	$7.44c^2 + 27.16cs + 24.79s^2$
$D^*\eta$	$1.30c^2 + 2.80cs + 1.51s^2$
$D_s^* K$	$0.01c^2 + 0.03cs + 0.02s^2$
$D_1(2430)^0\pi^0$	$5.38c^2 - 14.36cs + 9.58s^2$
$D_1(2430)^+\pi^-$	$10.39c^2 - 27.76cs + 18.55s^2$
$D_1(2420)^0\pi^0$	$2.51c^2 + 14.87cs + 22.41s^2$
$D_1(2420)^+\pi^-$	$4.78c^2 + 28.47cs + 42.96s^2$
$D_2(2460)^0\pi^0$	$(0.79c^2 + 0.98cs + 0.31s^2) \times 10^{-3}$
$D_2(2460)^+\pi^-$	$(0.73c^2 + 0.90cs + 0.28s^2) \times 10^{-3}$
$\Gamma_t = 36.28c^2 + 39.82cs + 228.90s^2$	

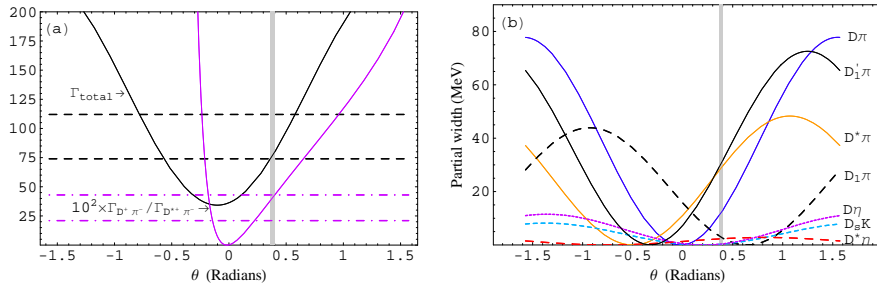


Figure 1: Decay widths and branching ratio  $\Gamma(D^+\pi)/\Gamma(D^{*+}\pi^-)$  of  $D(2600)$  versus  $\theta$ . The horizontal dashed (dot-dashed) lines indicate the upper and lower values of the experimental data on the total width (branching ratio).  $\Gamma(D_s^* K)$  and  $\Gamma(D_2(2460)\pi)$  are tiny and not shown.

The  $D(M_X)$  is expected to have a mass of about 2.77 GeV according to  $M_X^2 = M_{D(2^3S_1)}^2 + M_{D(1^3D_1)}^2 - M_{D(2600)}^2$ . Other approaches predicted that the  $D(M_X)$  would lie in about  $2.7 \sim 2.8$  GeV (see Table 1). The total width and branching ratio  $\Gamma(D^+\pi^-)/\Gamma(D^{*+}\pi^-)$  of  $D(M_X)$  as functions of the initial state mass  $M_X$  and the mixing angle  $\theta$  are illustrated in Fig. 2. The  $M_X$  is restricted to be  $2700 \sim 2800$  MeV and  $\theta$  is restricted to be  $0.364 \sim 0.4$  radians.

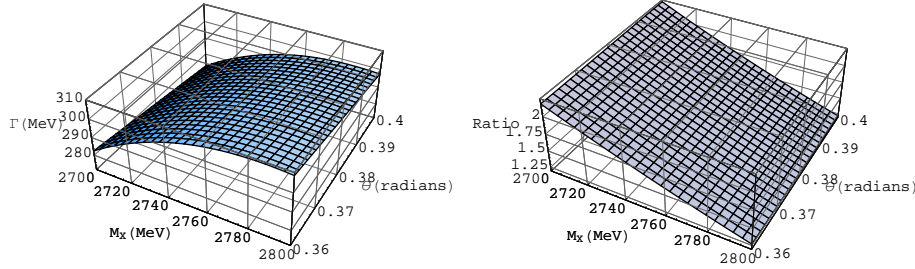


Figure 2: Total width and branching ratio  $\Gamma(D^+\pi)/\Gamma(D^{*+}\pi^-)$  of  $D(M_X)$  versus  $M_X$  and  $\theta$ .

As can be seen in Fig. 2, with the variations of the initial state mass and the mixing angle, the total width of  $D(M_X)$  varies from about 280 to 310 MeV and the branching ratio  $\Gamma(D^+\pi)/\Gamma(D^{*+}\pi^-)$  varies from about 1.25 to 2.25. At around 2760 MeV, the lower limit of the  $D(M_X)$ 's total width is expected to be about  $140 \sim 144$  MeV. Clearly, both the predicted total width and  $\Gamma(D^+\pi)/\Gamma(D^{*+}\pi^-)$  of the  $D(M_X)$  are in disagreement with the data concerning the  $D(2750)$  or  $D(2760)$ , which makes the  $D(2600)$ 's partner assignment for the  $D(2750)$  or  $D(2760)$  unlikely. This conclusion has been reached by Zhong in a chiral quark model[16]. We shall discuss other possible assignments for the  $D(2750)$  and  $D(2760)$  in the next subsection.

#### D. $D(2750)$ and $D(2760)$

Since the  $1^-$  assignment for the  $D(2750)$  or  $D(2760)$  seems unlikely as mentioned above, as shown in Table 4, the remaining possible assignments of  $D(2760)$  include the  $D(2^3P_0)$  and  $D(1^3D_3)$ , and the possible assignments of  $D(2750)$  are the  $D(1^3D_3)$ ,  $D_2(1D)$ , and  $D'_2(1D)$ .

The decay widths of  $D(2760)$  as  $D(2^3P_0)$  or  $D(1^3D_3)$  are listed in Table 8. The width of  $D(1^3D_3)$  is predicted to be about 73 MeV, compatible with the measured  $\Gamma(D(2760)) = 60.9 \pm 5.6 \pm 3.1$  MeV. The study in a chiral quark model also leads to a similar result ( $\sim 68$

MeV)[16]. The  $D(1^3D_3)$  interpretation for the  $D(2760)$  therefore appears suitable. The width of  $D(2^3P_0)$  is predicted to be about 135 MeV, about 70 MeV higher than  $60.9 \pm 5.6 \pm 3.1$  MeV. However, the lower limit of the  $D(2^3P_0)$ 's total width is expected to be about 72 MeV, compatible with the measurement, which makes the  $D(2^3P_0)$  assignments for the  $D(2750)$  also plausible.

Table 8: Decay widths of  $D(2760)$  as  $D(2^3P_0)$  or  $D(1^3D_3)$  in MeV. A symbol“ $\times$ ” indicates that a decay mode is forbidden.

	$D(2^3P_0)$	$D(1^3D_3)$
Mode	$\Gamma_i$	$\Gamma_i$
$D^0\pi^0$	20.10	10.74
$D^+\pi^-$	40.71	20.92
$D_s K$	17.84	0.82
$D\eta$	13.95	1.77
$D^{*0}\pi^0$	$\times$	10.42
$D^{*+}\pi^-$	$\times$	20.29
$D^*\eta$	$\times$	0.76
$D_s^* K$	$\times$	0.21
$D_1(2430)^0\pi^0$	12.25	0.72
$D_1(2430)^+\pi^-$	24.29	1.41
$D_1(2420)^0\pi^0$	2.14	0.02
$D_1(2420)^+\pi^-$	4.27	0.03
$D_2(2460)^0\pi^0$	$\times$	0.77
$D_2(2460)^+\pi^-$	$\times$	1.51
$D\omega$	$\times$	0.65
$D^0\rho^0$	$\times$	0.78
$D^+\rho^-$	$\times$	1.37
	$\Gamma_t = 135.54$	$\Gamma_t = 73.17$

The decay widths of  $D(2750)$  as  $D(1^3D_3)$ ,  $D'_2(1D)$ , and  $D'_2(1D)$  are listed in Table 9. The expressions of decay widths of  $D_2(1D)$  are not listed but the same as those of  $D'_2(1D)$  except that the  $\phi_{1D}^{c\bar{u}}$  is replaced by  $\phi_{1D}^{c\bar{u}} + \pi/2$ . The dependence of the total widths of  $D'_2(1D)$  and  $D'_2(1D)$  on the mixing angle  $\phi_{1D}^{c\bar{u}}$  is illustrated in Fig. 3. The total width of  $D(1^3D_3)$  is predicted to be about 67 MeV, consistent with the measured  $\Gamma(D(2750)) = 71 \pm 6 \pm 11$  MeV, which makes the  $D(1^3D_3)$  assignment for the  $D(2750)$  reasonable. The  $D_2(1D)$  is expected to be broader than the  $D'_1(2D)$ . The similar behavior exists in the  $[D_1(1P), D'_1(1P)]=[D_1(2430), D_1(2420)]$  system where the  $D_1(1P)$  is broader than the  $D'_1(1P)$ . From Fig. 3, one can see that, at 0.697 radians, the lower limit of the  $D_2(1D)$ 's total width is substantially larger than the upper limit

of the measurement, while the lower limit of the  $D'_2(1D)$ 's total width is close to the upper limit of the experiment. Therefore, if the  $D(2750)$  is indeed a  $2^-$  state, the favorable quarkonium assignment would be the  $D'_2(1D)$  rather than  $D_2(1D)$ .

Table 9: Decay widths of  $D(2750)$  as  $D(1^3D_3)$ ,  $D'_2(1D)$ , or  $D_2(1D)$  in MeV.  $c_1 \equiv \cos \phi_{1D}^{c\bar{u}}$  and  $s_1 \equiv \sin \phi_{1D}^{c\bar{u}}$ . Estimates of decay widths containing  $\phi_{1D}^{c\bar{u}}$  are given in terms of  $\phi_{1D}^{c\bar{u}} = 0.697$  radians. A symbol “ $\times$ ” indicates that a decay mode is forbidden.

	$D(1^3D_3)$	$D'_2(1D)$	$D_2(1D)$
Mode	$\Gamma_i$	$\Gamma_i$	
$D^0\pi^0$	10.13	$\times$	$\times$
$D^+\pi^-$	19.72	$\times$	$\times$
$D_s K$	0.71	$\times$	$\times$
$D\eta$	1.59	$\times$	$\times$
$D^{*0}\pi^0$	9.66	$29.36c_1^2 - 20.33c_1s_1 + 25.21s_1^2 = 17.65$	36.93
$D^{*+}\pi^-$	18.81	$58.66c_1^2 - 42.04c_1s_1 + 50.07s_1^2 = 34.43$	74.30
$D^{*}\eta$	0.63	$12.67c_1^2 - 18.89c_1s_1 + 8.81s_1^2 = 0.27$	19.70
$D_s^* K$	0.16	$0.11c_1^2 + 0.27c_1s_1 + 0.17s_1^2 = 1.78$	0.01
$D_1(2430)^0\pi^0$	0.60	$0.23c_1^2 - 0.12c_1s_1 + 0.02s_1^2 = 0.08$	0.17
$D_1(2430)^+\pi^-$	1.16	$0.45c_1^2 - 0.24c_1s_1 + 0.03s_1^2 = 0.16$	0.32
$D_1(2420)^0\pi^0$	0.01	$1.41c_1^2 + 0.84c_1s_1 + 0.12s_1^2 = 1.29$	0.24
$D_1(2420)^+\pi^-$	0.02	$2.69c_1^2 + 1.59c_1s_1 + 0.23s_1^2 = 2.46$	0.46
$D_2(2460)^0\pi^0$	0.60	$36.83c_2^2 - 60.60c_1s_1 + 25.26s_1^2 = 2.23$	59.86
$D_2(2460)^+\pi^-$	1.18	$73.99c_2^2 - 121.74c_1s_1 + 50.71s_1^2 = 4.48$	120.23
$D\omega$	0.47	$18.47c_1^2 + 28.83c_1s_1 + 12.59s_1^2 = 30.24$	0.82
$D^0\rho^0$	0.57	$13.35s_1^2 + 30.25c_1s_1 + 19.52c_1^2 = 31.87$	1.00
$D^+\rho^-$	0.99	$37.43c_1^2 + 58.30c_1s_1 + 25.53s_1^2 = 61.22$	1.74
$D_0(2400)^0\pi^0$	$\times$	$0.47c_1^2 + 0.86c_1s_1 + 0.39s_1^2 = 0.86$	0.002
$D_0(2400)^+\pi^-$	$\times$	$0.33c_1^2 + 0.75c_1s_1 + 0.43s_1^2 = 0.74$	0.02
$\Gamma_t = 67.01 \quad \Gamma_t = 293.22c_1^2 - 141.35c_1s_1 + 213.28s_1^2 = 189.70 \quad \Gamma_t = 315.81$			

The ratio  $\frac{\Gamma(D(2760) \rightarrow D^+\pi^-)}{\Gamma(D(2750) \rightarrow D^{*+}\pi^-)}$  is independent of the  $\gamma$  and therefore is crucial to further clarify the possible interpretations for the  $D(2760)$  and  $D(2750)$ . The predicted  $\frac{\Gamma(D(2760) \rightarrow D^+\pi^-)}{\Gamma(D(2750) \rightarrow D^{*+}\pi^-)}$  for possible combinations are shown in Table 10. It is obvious that only under the identification of the  $[D(2760), D(2750)]$  as the  $[D(1^3D_3), D'_2(1D)]$  which leads to  $\frac{\Gamma(D(2760) \rightarrow D^+\pi^-)}{\Gamma(D(2750) \rightarrow D^{*+}\pi^-)} = 0.6$ , the measured branching ratio of  $0.42 \pm 0.05 \pm 0.11$  can be reasonably accounted for. Therefore the  $[D(1^3D_3), D'_2(1D)]$  assignment for the  $[D(2760), D(2750)]$  is agreeable. The calculations preformed by Wang in the heavy quark effective theory[17] also support this picture. The Babar Collaboration suggested that  $D(2760)$  and  $D(2750)$  may be the  $D$ -wave states, favoring our present assignment. For the  $D(1^3D_3)$ , the main decay modes are  $D\pi$ ,  $D^*\pi$ ,  $D\rho$ ,  $D_2(2460)K$ ,

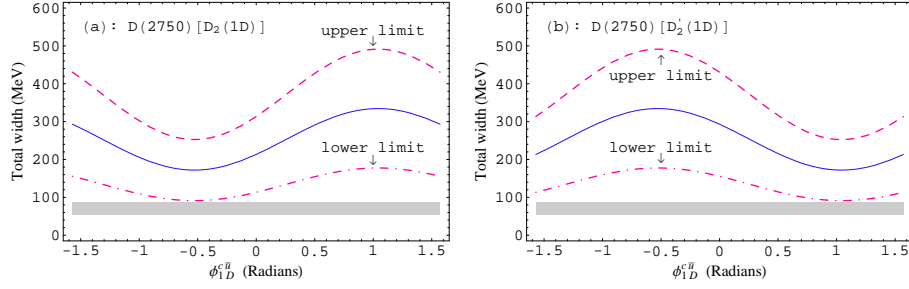


Figure 3: The total width of  $D(2750)$  as the  $2^-$  state versus the mixing angle. The shadow indicates the experimentally allowed range.

and  $D_1(2430)K$ , while for the  $D'_2(1D)$  they are  $D^*\pi$ ,  $D\omega$ ,  $D\rho$ , and  $D_2(2460)K$ . It is expected that  $\Gamma(D\rho)/\Gamma(D^*\pi)$  for the  $D(1^3D_3)$  and  $D'_2(1D)$  are about 1.8 and 0.07, respectively. Further experimental information on these two states in  $D^*\pi$ ,  $D\omega$ , and  $D\rho$  channels can further test the present assignments for  $D(2760)$  and  $D(2750)$ .

Table 10:  $\frac{\Gamma(D(2760) \rightarrow D^+\pi^-)}{\Gamma(D(2750) \rightarrow D^{*+}\pi^-)}$  for possible combinations.

$[D(2760), D(2750)]$	$\frac{\Gamma(D(2760) \rightarrow D^+\pi^-)}{\Gamma(D(2750) \rightarrow D^{*+}\pi^-)}$
$[D(2^3P_0), D(1^3D_3)]$	2.16
$[D(2^3P_0), D'_2(1D)]$	1.18
$[D(1^3D_3), D(1^3D_3)]$	1.11
$[D(1^3D_3), D'_2(1D)]$	0.60

The  $D(2750)$  signal observed in  $D^*\pi$  is very similar to the  $D(2760)$  signal observed in  $D\pi$ , their mass and width values differ by  $2.6\sigma$  and  $1.5\sigma$ [2]. Therefore, it is likely that the  $D(2760)$  and  $D(2750)$  refer to the same resonance. If so, since the  $1^-$  interpretation for the  $D(2760)$  or  $D(2750)$  can be excluded as discussed previously, the only one possible quarkonium assignment would be that they are the same  $D(1^3D_3)$ , although the ratio of  $\Gamma(D^+\pi^-)/\Gamma(D^{*+}\pi^-)$  is somewhat larger than the measured  $0.42 \pm 0.05 \pm 0.11$ .<sup>4</sup> Clearly, the further search of the  $D(2750)$  in the  $D\pi$ ,  $D_sK$ ,  $D\eta$ , and  $D_0(2400)\pi$  channels is crucial to discriminate the  $2^-$  and  $3^-$  assignments for the  $D(2750)$  because a  $3^- c\bar{n}$  state is forbidden to decay into  $D_0(2400)\pi$  while a  $2^- c\bar{n}$  state is forbidden to decay into  $D\pi$ ,  $D_sK$ , and  $D\eta$ . Also, the  $\Gamma(D\rho)/\Gamma(D^*\pi)$  for the  $D'_2(1D)$  is

<sup>4</sup>Under the  $D(1^3D_3)$  assignment, this ratio is expected to be about 1.0 at the initial state mass of  $(2763.3 + 2752.4)/2$  MeV. The similar result of about 0.9 is also obtained in a  $^3P_0$  model[15]. The predictions from the chiral quark model[16] and the heavy quark effective theory[17] are 1.58 and 1.94, respectively.

remarkably different from that for the  $D(1^3D_3)$ , therefore the experimental information on the  $D(2750)$  in the  $D\rho$  and  $D\omega$  is also important to differentiate these two possible interpretations for the  $D(2750)$ .

In summary, if the  $D(2750)$  and  $D(2760)$  are confirmed to be the same resonance, they would be the  $D(1^3D_3)$ ; otherwise, the favorable interpretation would be that the  $D(2750)$  and  $D(2760)$  are the  $D'_2(1D)$  and  $D(1^3D_3)$ , respectively. To distinguish these two possibilities, further experimental studies on these two states are needed. Below we turn to the charmed-strange states.

### E. $D_{s1}(2710)$ and $D_{sJ}(2860)$

In the 2S-1D mixing scenario, the eigenvectors of  $D_{s1}(2710)$  and its partner  $D_{s1}(M_Y)$  can be written as

$$|D_{s1}(2710)\rangle = \cos\theta_1|2^3S_1\rangle - \sin\theta_1|1^3D_1\rangle, \quad (18)$$

$$|D_{s1}(M_Y)\rangle = \sin\theta_1|2^3S_1\rangle + \cos\theta_1|1^3D_1\rangle, \quad (19)$$

where the  $\theta_1$  is the  $D_s(2^3S_1)$ - $D_s(1^3D_1)$  mixing angle and  $M_Y$  denotes the mass of the physical state  $D_{s1}(M_Y)$ .

The decay widths of  $D_{s1}(2710)$  are listed in Table 11. The variations of decay widths and  $\Gamma(D^*K)/\Gamma(DK)$  with the mixing angle  $\theta_1$  are illustrated in Fig. 4. Clearly, with  $1.06 \leq \theta_1 \leq 1.34$  radians, both the total width and  $\Gamma(D^*K)/\Gamma(DK)$  of  $D_{s1}(2710)$  can be well reproduced (see Fig. 4 (a)). Also, in this mixing angle range, the main decay modes are  $DK$  and  $D^*K$  (see Fig. 4 (b)), in accord with the observation of the  $D_{s1}(2710)$  in the  $DK$  and  $D^*K$ . Therefore, the picture of  $D_{s1}(2710)$  being in fact a mixture of the  $D_s(2^3S_1)$  and  $D_s(1^3D_1)$  seems convincing. The studies in a chiral quark model[13] and a  $^3P_0$  model[14] also favor this interpretation. Future experimental information on the  $D_{s1}(2710)$  in the remaining channels  $D_s\eta$  and  $D_s^*\eta$  can provide a consistent check for this assignment.

According to  $M_Y^2 = M_{D_s(2^3S_1)}^2 + M_{D_s(1^3D_1)}^2 - M_{D_{s1}(2710)}^2$ , the  $D(M_Y)$  is expected to have a mass of about 2.81 GeV. Other approaches predicted  $M_Y \simeq 2.8 \sim 2.9$  GeV (see Table 2). The total width and the branching ratio  $\Gamma(D^*K)/\Gamma(DK)$  for the  $D_{s1}(M_Y)$  as functions of the initial



Table 11: Decay widths of  $D_{s1}(2710)$  and  $D_{sJ}(2860)$  as the  $1^-$  states.  $c_2 \equiv \cos \theta_1$ , and  $s_2 \equiv \sin \theta_1$ . A dash indicates that a decay mode is below threshold.

	$D_{s1}(2710)$	$D_{sJ}(2860)$
Mode	$\Gamma_i$	$\Gamma_i$
$D^0 K^+$	$2.29c_2^2 - 24.74c_2s_2 + 66.71s_2^2$	$60.22c_2^2 - 6.47c_2s_2 + 0.17s_2^2$
$D^+ K^0$	$2.49c_2^2 - 25.79c_2s_2 + 66.54s_2^2$	$61.17c_2^2 - 4.89c_2s_2 + 0.10s_2^2$
$D_s \eta$	$0.49c_2^2 - 3.69c_2s_2 + 6.90s_2^2$	$10.96c_2^2 + 2.64c_2s_2 + 0.16s_2^2$
$D^{*0} K^+$	$21.81c_2^2 + 49.05c_2s_2 + 27.57s_2^2$	$33.93c_2^2 - 38.36c_2s_2 + 10.84s_2^2$
$D^{*+} K^0$	$21.83c_2^2 + 48.55c_2s_2 + 26.99s_2^2$	$34.15c_2^2 - 36.69c_2s_2 + 11.53s_2^2$
$D_s^* \eta$	$0.79c_2^2 + 1.59c_2s_2 + 0.80s_2^2$	$4.51c_2^2 - 7.20c_2s_2 + 2.87s_2^2$
$D^0 K^{*+}$	—	$25.22c_2^2 - 67.82c_2s_2 + 45.58s_2^2$
$D^+ K^{*0}$	—	$23.32c_2^2 - 63.30c_2s_2 + 42.94s_2^2$
	$\Gamma_t = 49.72c_2^2 + 44.95c_2s_2 + 195.52s_2^2$	$\Gamma_t = 253.49c_2^2 - 225.07c_2s_2 + 114.20s_2^2$

state mass  $M_Y$  and the mixing angle  $\theta_1$  are illustrated in Fig. 5. The  $M_Y$  is restricted to be  $2800 \sim 2900$  MeV and the  $\theta_1$  is restricted to be  $1.06 \sim 1.34$  radians. With the variations of the initial state mass and the mixing angle, the total width of  $D_{s1}(M_Y)$  varies from about 40 to 70 MeV and the  $\Gamma(D^*K)/\Gamma(DK)$  varies from about 0.04 to 2.71.

Both the predicted mass and width of  $D_{s1}(M_Y)$  are consistent with those of  $D_{sJ}(2860)$ . Therefore, if  $D_{sJ}(2860)$  is a  $1^-$  state, it would be a natural candidate for the  $D_{s1}(M_Y)$ . Under this picture, the numerical results for the decays widths of  $D_{sJ}(2860)$  are listed in Table 11, and the dependence of the total width as well as  $\Gamma(D^*K)/\Gamma(DK)$  on the mixing angle  $\theta_1$  is illustrated in Figs.4. It is clear that both the total width and  $\Gamma(D^*K)/\Gamma(DK)$  of  $D_{sJ}(2860)$  can be well reproduced with  $1.29 \leq \theta_1 \leq 1.33$  radians, just lying on the range of  $1.06 \leq \theta_1 \leq 1.34$  radians (see 4(c)). Also, in this mixing angle range, the main decay modes are  $DK^*$ ,  $D^*K$  and  $DK$ , consistent with the observation of the  $D_{sJ}(2860)$  in  $DK$  and  $D^*K$ . Therefore, the identification of  $D_{sJ}(2860)$  as the partner of  $D_{s1}(2710)$  appears convincing. The study in a  $^3P_0$  model[14] also favors this assignment.

The  $D_{sJ}(2860)$  could also be the  $D_s(1^3D_3)$  as shown in Table 4. In this case, the decay widths are listed in Table 12. It is expected that  $\Gamma \simeq 77$  MeV and branching ratio  $\Gamma(D^*K)/\Gamma(DK) \simeq 0.8$ . The predicted  $\Gamma(D^*K)/\Gamma(DK) \simeq 0.8$  is consistent with the measurement. The predicted total width is about 20 MeV larger than the experiment. The lower limit of the predicted width is about 41 MeV, consistent with the experiment. The main decay modes are  $DK$  and  $D^*K$ , in

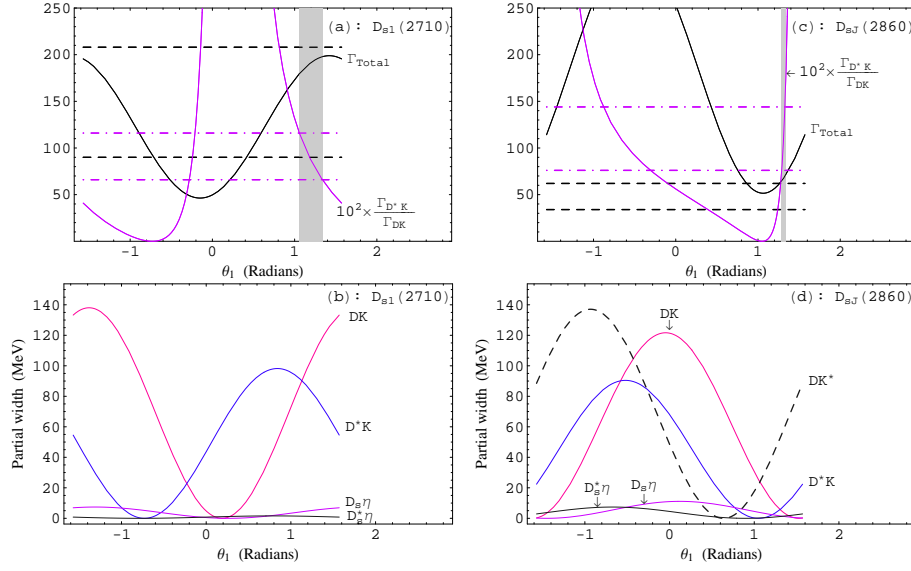


Figure 4: Total widths and  $\Gamma(D^*K)/\Gamma(DK)$  of  $D_{s1}(2710)$  and  $D_{sJ}(2860)$  versus  $\theta_1$ . The horizontal dashed lines indicate the upper and lower limits of experimental data.

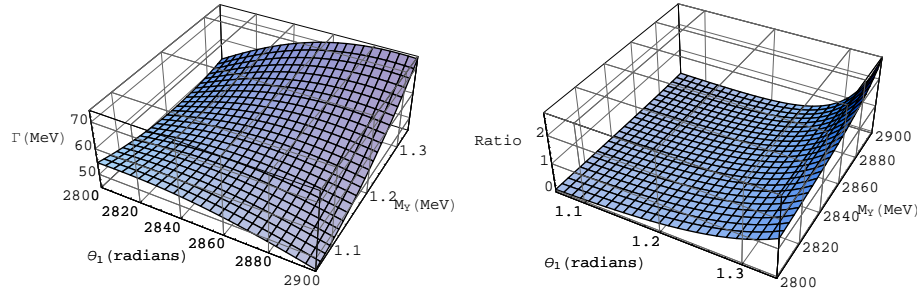


Figure 5: Total width and branching ratio  $\Gamma(D^*K)/\Gamma(DK)$  of  $D_{s1}(M_X)$  versus  $M_Y$  and  $\theta_1$ .

accord with the observation. The  $D_s(1^3D_3)$  interpretation for the  $D_{sJ}(2860)$  thus seems likely. This assignment is also favored by the studies in the  $^3P_0$  model[14] and lattice QCD[40].

Both the  $1^-$  and  $3^-$  interpretations for the  $D_{sJ}(2860)$  appear reasonable. The available experimental information on the  $D_{sJ}(2860)$  is not enough to discriminate these two possibilities. However, the differences between the  $1^-$  and  $3^-$  interpretations are evident. For example, for the  $3^-$  assignment,  $\Gamma(DK)/\Gamma(D_s^*\eta) \simeq 119.7$ ,  $\Gamma(DK)/\Gamma(D_s\eta) \simeq 45.1$ , and  $\Gamma(DK)/\Gamma(DK^*) \simeq 18.2$ , while for the  $1^-$  assignment,  $\Gamma(DK)/\Gamma(D_s^*\eta) \simeq 3.5 \sim 6.1$ ,  $\Gamma(DK)/\Gamma(D_s\eta) \simeq 3.3 \sim 3.9$ , and  $\Gamma(DK)/\Gamma(DK^*) \simeq 0.08 \sim 0.13$ . Further experimental information on the  $D_{sJ}(2860)$  in  $D_s\eta$ ,

Table 12: Decay widths of  $D_{sJ}(2860)$  as  $D_s(1^3D_3)$  in MeV.

$D^0 K^+$	$D^+ K^0$	$D_s \eta$	$D^{*0} K^+$	$D^{*+} K^0$	$D_s^* \eta$	$D^0 K^{*+}$	$D^+ K^{*0}$	Total
21.38	20.53	0.93	16.18	15.40	0.35	1.31	0.99	77.05

$D_s^* \eta$ , and  $DK^*$  channels is crucial to distinguish these two possible assignments.

## F. $D_{sJ}(3040)$

The decay widths of  $D_{sJ}(3040)$  as  $D_{s1}(2P)$  or  $D'_{s1}(2P)$  are listed in Table 13. The expressions of the decay widths of  $D'_{s1}(2P)$  are not listed but the same as those of the  $D_{s1}(2P)$  except that the  $\phi_{2P}^{c\bar{s}}$  is replaced by  $\phi_{2P}^{c\bar{s}} + \pi/2$ . The dependence, of the total width of  $D_{sJ}(3040)$  as  $1^+$  state, on the mixing angle  $\phi_{2P}^{c\bar{s}}$  and  $\beta_A$  are illustrated in Fig. 6 and Fig. 7.

As can be seen in Fig. 6, at  $\phi_{2P}^{c\bar{s}} = 0.564$  radians, the predicted  $\Gamma(D_{s1}(2P))$  and  $\Gamma(D'_{s1}(2P))$  are close to the upper and lower limits of the experimental data of  $239 \pm 35^{+46}_{-42}$  MeV, respectively. The similar behavior also exists at about  $\beta_A = 306$  MeV, as shown in Fig. 7. Within the theoretical and experimental errors, the predicted total widths for both  $D_{s1}(2P)$  and  $D'_{s1}(2P)$  are comparable with the experiment. Therefore, both the  $D_{s1}(2P)$  and  $D'_{s1}(2P)$  assignments for the  $D_{sJ}(3040)$  seem likely based on its measured total width. It should be noted that since the experimental errors of  $\Gamma(D_{sJ}(3040))$  is large, the improved measurement of  $\Gamma(D_{sJ}(3040))$  is needed to confirm our present assignment.

Also, Fig. 7 indicates that in the vicinity of initial state  $\beta = 300$  ( $270 \leq \beta_A \leq 330$  MeV), the  $D_{s1}(2P)$  is expected to be about  $100 \sim 150$  MeV broader than the  $D'_{s1}(2P)$  in width, which is consistent with the prediction from the heavy quark effective theory. In the framework of the heavy quark effective theory, the  $D_{s1}(2P)$  is the  $1^+$  state existing in  $S = (0^+, 1^+)$  doublet while  $D'_{s1}(2P)$  corresponds to the  $1^+$  state of  $T = (1^+, 2^+)$  doublet, and the  $1^+$  state of  $S$  doublet is predicted to be broader than the one of  $T$  doublet[12, 39]. The similar conclusion has been reached in calculations from the  $^3P_0$  model[12] and the chiral quark model[13].

For the  $D_{s1}(2P)$ , the main decay modes are  $D_2(2460)K$ ,  $D^*K$ ,  $D^*K^*$ ,  $DK^*$ , and  $D_0(2400)K$ , while for the  $D'_{s1}(2P)$  they are  $D^*K^*$ ,  $DK^*$ ,  $D^*K$ ,  $D_0(2400)K$ ,  $D_1(2420)K$ , and  $D_2(2460)K$ . The branching ratios  $\Gamma(D^*K^*)/\Gamma(D^*K)$ ,  $\Gamma(DK^*)/\Gamma(D^*K)$  and  $\Gamma(D_2(2460)K)/\Gamma(D^*K)$  are

expected to be respectively about 0.9, 0.8, and 1.1 for the  $D_{s1}(2P)$ , while about 5.0, 2.0, and 0.4 for the  $D'_{s1}(2P)$ . The decay patterns for these two assignments are different. The additional experimental information on the branching ratios of  $D_{sJ}(3040)$  are important to discriminate these two possibilities.

Table 13: Decay widths of  $D_{sJ}(3040)$  as the  $D_{s1}(2P)$  or  $D'_{s1}(2P)$  in MeV.  $c_3 \equiv \cos \phi_{2P}^{c\bar{s}}$ ,  $s_3 \equiv \sin \phi_{2P}^{c\bar{s}}$ . Estimates of decay widths containing  $\phi_{2P}^{c\bar{s}}$  are given in terms of  $\phi_{2P}^{c\bar{s}} = 0.564$  radians.

Mode	$D_{s1}(2P)$	$D'_{s1}(2P)$
	$\Gamma_i$	$\Gamma_i$
$D^0 K^{*+}$	$25.33c_3^2 + 18.27c_3s_3 + 19.25s_3^2 = 31.85$	12.74
$D^+ K^{*0}$	$24.51c_3^2 + 16.28c_3s_3 + 19.08s_3^2 = 30.31$	13.27
$D_s \phi$	$0.45c_3^2 - 0.05c_3s_3 + 0.34s_3^2 = 0.39$	0.40
$D^{*0} K^+$	$14.92c_3^2 + 35.09c_3s_3 + 27.42s_3^2 = 34.35$	7.99
$D^{*+} K^0$	$14.91c_3^2 + 36.01c_3s_3 + 27.72s_3^2 = 34.84$	7.79
$D_s^* \eta$	$2.39c_3^2 + 6.84c_3s_3 + 4.90s_3^2 = 6.20$	1.10
$D^{*0} K^{*+}$	$31.08c_3^2 + 44.35s_3^2 = 34.59$	39.84
$D^{*+} K^{*0}$	$28.83c_3^2 + 40.77s_3^2 = 32.24$	37.36
$D_1(2430)^0 K^+$	$0.01c_3^2 - 0.21c_3s_3 + 2.08s_3^2 = 0.50$	1.59
$D_1(2430)^+ K^0$	$0.01c_3^2 - 0.21c_3s_3 + 1.99s_3^2 = 0.48$	1.52
$D_1(2420)^0 K^+$	$0.01c_3^2 - 0.37c_3s_3 + 6.74s_3^2 = 1.76$	4.99
$D_1(2420)^+ K^0$	$0.01c_3^2 - 0.38c_3s_3 + 6.77s_3^2 = 1.77$	5.01
$D_2(2460)^0 K^+$	$21.22c_3^2 + 40.71c_3s_3 + 21.47s_3^2 = 39.68$	3.00
$D_2(2460)^+ K^0$	$20.79c_3^2 + 40.05c_3s_3 + 21.07s_3^2 = 38.97$	2.89
$D_0(2400)^0 K^+$	$25.92c_3^2 + 1.23c_3s_3 + 0.01s_3^2 = 19.07$	6.86
$D_0(2400)^+ K^0$	$20.81c_3^2 - 1.05c_3s_3 + 0.01s_3^2 = 14.39$	6.43
$D_{s1}(2460)\eta$	$(0.05c_3^2 - 1.54c_3s_3 + 12.89s_3^2) \times 10^{-2} = 0.03$	0.10
$D_{s0}(2317)\eta$	$(431.34c_3^2 + 8.87c_3s_3 + 0.05s_3^2) \times 10^{-2} = 3.12$	1.19
	$\Gamma_t = 235.50c_3^2 + 192.29c_3s_3 + 243.11s_3^2 = 324.55$	$\Gamma_t = 154.06$

## IV. Radiative decays

It is well known that radiative transitions can probe the internal charge structure of hadrons, and therefore they will likely play an important role in determining the quantum numbers and hadronic structures of these new open-charm mesons. In this section, we shall evaluate the  $E1$  and  $M1$  transitions widths of these open-charm states.

The partial widths for the  $E1$  and  $M1$  transitions between the  $v = n \ 2S+1L_J$  and  $v' =$

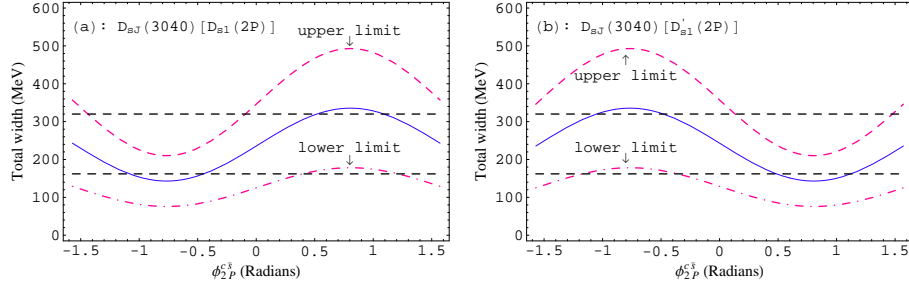


Figure 6: The total width of  $D_{sJ}(3040)$  as the  $1^+$  state versus the mixing angle. The horizontal dashed lines indicate the upper and lower limits of experimental data.

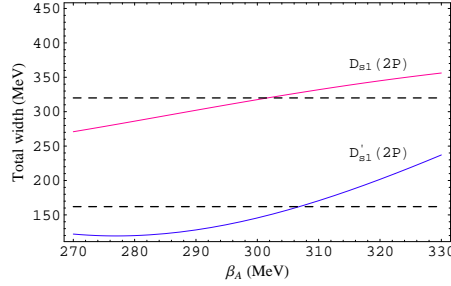


Figure 7: The total width of  $D_{sJ}(3040)$  as the  $1^+$  state versus the  $\beta_A$ . Here,  $\beta_{2^3P_1}$  is set to  $\beta_{2^1P_1}$ . The horizontal dashed lines indicate the upper and lower limits of experimental data.

$n'2S'+1L'_{J'}$ ,  $c\bar{q}$  states in the nonrelativistic quark model are given by[38, 41]

$$\Gamma_{E1}(v \rightarrow v' + \gamma) = \frac{4\alpha e_Q^2}{3} C_{fi} \delta_{SS'} |\langle v'|r|v \rangle|^2 \frac{E_\gamma^3 E_f}{M_i} \quad (20)$$

$$\Gamma_{M1}(v \rightarrow v' + \gamma) = \frac{\alpha e_Q'^2}{3} \frac{2J'+1}{2L+1} \delta_{LL'} \delta_{SS'\pm 1} \left| \langle v'|j_0 \left( \frac{E_\gamma r}{2} \right) |v \rangle \right|^2 \frac{E_\gamma^3 E_f}{M_i}, \quad (21)$$

where  $e_Q = \frac{m_q Q_c + m_c Q_q}{(m_q + m_c)}$ ,  $e'_Q = \frac{m_q Q_c + m_c Q_q}{(m_q m_c)}$ ,  $Q_c$  and  $Q_q$  denote the quark  $c$  and  $q$  charges in units of  $|e|$ , respectively.  $\alpha = 1/137$  is the fine-structure constant,  $E_\gamma$  is the final photon energy,  $E_f$  is the energy of the final state  $n'2S'+1L'_{J'}$ ,  $M_i$  is the initial state mass, and the angular matrix element  $C_{fi}$  is

$$C_{fi} = \text{Max}(L, L')(2J'+1) \left\{ \begin{matrix} L' & J' & S \\ J & L & 1 \end{matrix} \right\}^2. \quad (22)$$

The wave functions used to evaluate the matrix element  $\langle v'|r|v \rangle$  and  $\langle v'|j_0(E_\gamma r/2)|v \rangle$  are obtained from the nonrelativistic quark model (11). According to the PDG[26], the well established  $D$  and  $D_s$  states include the  $D$ ,  $D_s$ ,  $D^*$ ,  $D_s^*$ ,  $D_0(2400)$ ,  $D_{s0}(2317)$ ,  $D_1(2430)$ ,  $D_1(2420)$ ,  $D_{s1}(2460)$ ,  $D_{s1}(2536)$ ,  $D_2(2460)$ , and  $D_{s2}(2573)$ . Therefore, we only consider the processes

where the final states contain the ground  $S$  and  $P$ -wave open-charm mesons. The resulting  $E1$  transitions widths of these open-charm states for the favorable assignments mentioned in above sections together with the photon energies are given in Tables 14-17. The  $M1$  transitions widths are given in Table 18.

As can be seen in Table 15, the  $D_1(2420)\gamma$  and  $D_1(2430)\gamma$  are clearly of great interest to discriminate the  $2^-$  and  $3^-$  interpretations for the  $D(2750)$ , since these modes are forbidden for a  $3^-$  state while allowable for a  $2^-$  state. Especially, the  $\Gamma(D'_2(1D) \rightarrow D_1(2420)\gamma)$  is expected to be about 757 keV and thus becomes an experimentally promising process.

Similarly, from Table 16, the experimental information on the  $D_{sJ}(2860)$  in the  $D_{s0}(2317)\gamma$ ,  $D_{s1}(2459)\gamma$ , and  $D_{s1}(2535)\gamma$  would be important to discriminate the  $1^-$  and  $3^-$  interpretations since these decay modes are forbidden for the  $3^-$  state while allowable for the  $1^-$  state.

As for the  $M1$  transitions, experimental study on the ratio  $R = \frac{\mathcal{B}(D_{sJ}(3040) \rightarrow D_{s1}(2460))}{\mathcal{B}(D_{sJ}(3040) \rightarrow D_{s1}(2535))}$  would be useful to discriminate the  $D_{s1}(2P)$  and  $D'_{s1}(2P)$  interpretations since it is expected that  $R(D_{s1}(2P)) \approx 11.7$  while  $R(D'_{s1}(2P)) \approx 1.3$ .

Table 14:  $E1$  transitions widths of  $D(2550)$  and  $D(2600)$ .  $E_\gamma$  in MeV,  $\Gamma$  in keV,  $c \equiv \cos \theta$ , and  $s \equiv \sin \theta$ . Estimates of decay widths containing  $\theta$  are given in terms of  $\theta = 0.4$  radians. A symbol “ $\times$ ” indicates that a decay mode is forbidden.

Final meson	$D(2550)[2^1S_0]$			$D(2600)[2S-1D]$	
	$E_\gamma$	$\Gamma$	$E_\gamma$	$\Gamma$	
$D_2(2460)^0$	$\times$	$\times$	143	$86.4c^2 + 32.7cs + 3.1s^2 \simeq 85.5$	
$D_0(2400)^0$	$\times$	$\times$	283	$125.8c^2 + 475.6cs + 449.6s^2 \simeq 345.5$	
$D_1(2430)^0$	110	76.0	175	$11.8c^2 + 22.3cs + 10.6s^2 \simeq 19.6$	
$D_1(2420)^0$	114	12.3	180	$166.2c^2 + 87.9cs + 78.6s^2 \simeq 184.3$	

Table 15:  $E1$  transitions widths of  $D(2760)$  and  $D(2750)$ .  $E_\gamma$  in MeV,  $\Gamma$  in keV,  $c_1 \equiv \cos \phi_{2D}^{c\bar{u}}$ , and  $s_1 \equiv \sin \phi_{1D}^{c\bar{u}}$ . Estimates of decay widths containing  $\phi_{1D}^{c\bar{u}}$  are given in terms of  $\phi_{1D}^{c\bar{u}} = 0.697$  radians. A symbol “ $\times$ ” indicates that a decay mode is forbidden.

Final meson	$E_\gamma$	$D(2750)$		$D(2760)$	
		$\Gamma[D'_2(1D)]$	$\Gamma[1^3D_3]$	$E_\gamma$	$\Gamma[1^3D_3]$
$D_2(2460)^0$	276	$188.5c_1^2 \simeq 110.8$	753.9	286	834.2
$D_0(2400)^0$	$\times$	$\times$	$\times$	$\times$	$\times$
$D_1(2430)^0$	306	$96.2c_1^2 - 578.5c_1s_1 + 869.4s_1^2 \simeq 130.1$	$\times$	$\times$	$\times$
$D_1(2420)^0$	310	$693.4c_1^2 - 601.3c_1s_1 + 130.4s_1^2 \simeq 757.3$	$\times$	$\times$	$\times$

Table 16:  $E1$  transitions widths of  $D_{s1}(2710)$  and  $D_{sJ}(2860)$ .  $E_\gamma$  in MeV,  $\Gamma$  in keV,  $c_2 \equiv \cos \theta_1$ , and  $s_2 \equiv \sin \theta_1$ . Estimates of decay widths containing  $\theta_1$  are given in terms of  $\theta_1 = 1.31$  radians. A symbol “ $\times$ ” indicates that a decay mode is forbidden.

Final meson	$E_\gamma$	$D_{s1}(2710)$	$E_\gamma$	$D_{sJ}(2860)$	$\Gamma[1^3D_3]$
		$\Gamma[2S-1D]$		$\Gamma[2S-1D]$	
$D_{s2}(2573)$	134	$0.4c_2^2 + 0.2c_2s_2 + 0.02s_2^2 \simeq 0.1$	275	$0.1c_2^2 - 1.4c_2s_2 + 3.7s_2^2 \simeq 3.1$	4.6
$D_{s0}(2317)$	364	$1.6c_2^2 + 6.1c_2s_2 + 5.7s_2^2 \simeq 6.9$	492	$13.6c_2^2 - 14.5c_2s_2 + 3.9s_2^2 \simeq 0.9$	$\times$
$D_{s1}(2460)$	239	$0.3c_2^2 + 0.5c_2s_2 + 0.2s_2^2 \simeq 0.3$	374	$0.8c_2^2 - 1.7c_2s_2 + 0.9s_2^2 \simeq 0.5$	$\times$
$D_{s1}(2536)$	169	$0.4c_2^2 + 0.8c_2s_2 + 0.4s_2^2 \simeq 0.6$	308	$2.2c_2^2 - 4.7c_2s_2 + 2.5s_2^2 \simeq 1.3$	$\times$

Table 17:  $E1$  transitions widths of  $D_{sJ}(3040)$ .  $E_\gamma$  in MeV,  $\Gamma$  in keV,  $c_3 \equiv \cos \phi_{2P}^{c\bar{s}}$ , and  $s_3 \equiv \sin \phi_{2P}^{c\bar{s}}$ . Estimates of decay widths containing  $\phi_{2P}^{c\bar{s}}$  are given in terms of  $\phi_{2P}^{c\bar{s}} = 0.564$  radians.

Final meson	$E_\gamma$	$D_{sJ}(3040)$	
		$\Gamma[D_{s1}(2P)]$	$\Gamma[D'_{s1}(2P)]$
$D_s(1969)$	886	$1.6c_3^2 \simeq 1.1$	$1.6s_3^2 \simeq 0.5$
$D_s^*(2112)$	789	$0.5s_3^2 \simeq 0.1$	$0.5c_3^2 \simeq 0.4$
$D_{s2}(2573)$	435	$0.6s_3^2 \simeq 0.2$	$0.6c_3^2 \simeq 0.4$
$D_{s0}(2317)$	640	$1.5s_3^2 \simeq 0.4$	$1.5c_3^2 \simeq 1.1$
$D_{s1}(2460)$	528	$2.1c_3^2 + 1.0c_3s_3 + 0.1s_3^2 \simeq 1.9$	$2.1s_3^2 - 1.0c_3s_3 + 0.1c_3^2 \simeq 0.2$
$D_{s1}(2536)$	466	$0.3c_3^2 - 0.7c_3s_3 + 0.4s_3^2 \simeq 0.01$	$0.3s_3^2 + 0.7c_3s_3 + 0.4c_3^2 \simeq 0.7$

## V. Summary and conclusion

The discovery of  $D(2550)$ ,  $D(2600)$ ,  $D(2750)$ ,  $D(2760)$ ,  $D_{s1}(2710)$ ,  $D_{sJ}(2860)$ , and  $D_{sJ}(3040)$  provides a good opportunity to test our present understanding of charmed mesons and is also of importance to further establish the  $D$  and  $D_s$  spectra. We are trying to shed some light on the natures of these open-charm states by investigating their masses and decays in the nonrelativistic constituent quark model.

We first calculated the charmed meson spectrum in the nonrelativistic constituent quark model. The overall agreement between our predicted masses and those from other approaches such as the Blankenbecler-Sugar equation and the relativistic quark models turns out to be satisfactory. According to the observed decay modes and by comparing the measured masses with our predictions, we presented the possible assignments of these newly observed open-charm states.

Mass spectra alone are insufficient to determine the quantum numbers of these open-charm

Table 18:  $M1$  transitions widths.  $E_\gamma$  in MeV,  $\Gamma$  in keV, Estimates of decay widths containing mixing angles are given in terms of the same values used in  $E1$  transitions.

Mode	$E_\gamma$	$\Gamma$
$D(2550)^0[2^1S_0] \rightarrow D^{*0}\gamma$	477	13.9
$D(2600)^0[2S-1D] \rightarrow D^0\gamma$	638	$97.3c^2 = 82.6$
$D_{s1}(2710)[2S-1D] \rightarrow D_s\gamma$	640	$0.47c_2^2 = 0.03$
$D_{sJ}(2860)[2S-1D] \rightarrow D_s\gamma$	754	$0.88s_2^2 = 0.82$
$D_{sJ}(3040)[D_{s1}(2P)] \rightarrow D_{s1}(2460)$	528	$0.01c_3^2 + 0.08c_3s_3 + 0.1s_3^2 = 0.07$
$D_{sJ}(3040)[D'_{s1}(2P)] \rightarrow D_{s1}(2460)$	528	$0.01s_3^2 - 0.08c_3s_3 + 0.1c_3^2 = 0.04$
$D_{sJ}(3040)[D_{s1}(2P)] \rightarrow D_{s1}(2536)$	466	$0.03c_3^2 - 0.04c_3s_3 + 0.01s_3^2 = 0.006$
$D_{sJ}(3040)[D'_{s1}(2P)] \rightarrow D_{s1}(2536)$	466	$0.03s_3^2 + 0.04c_3s_3 + 0.01c_3^2 = 0.03$
$D_{sJ}(3040)[D_{s1}(2P)] \rightarrow D_{s0}(2317)$	640	$0.09c_3^2 = 0.06$
$D_{sJ}(3040)[D'_{s1}(2P)] \rightarrow D_{s1}(2317)$	640	$0.09s_3^2 = 0.03$
$D_{sJ}(3040)[D_{s1}(2P)] \rightarrow D_{s2}(2573)$	435	$0.01c_3^2 = 0.007$
$D_{sJ}(3040)[D'_{s1}(2P)] \rightarrow D_{s2}(2573)$	435	$0.01s_3^2 = 0.003$

states. Studies on the decay dynamics of these states are needed. We therefore further evaluated the strong and  $E1$  and  $M1$  radiative decays of these open-charm states for possible assignments.

Comparing our predictions with the experiment, we conclude that (1) if the  $D(2550)$  is indeed the  $D(2^1S_0)$  state, its width could be overestimated experimentally; (2) the  $D(2600)$  and  $D_{s1}(2710)$  can be identified as the  $2^3S_1$ - $1^3D_1$  mixtures; (3) if the  $D(2750)$  and  $D(2760)$  are the same state, they could be interpreted as the  $D(1^3D_3)$ ; otherwise, they could be assigned as the  $D(1^3D_3)$  and  $D'_2(1D)$ , respectively; (4) both the  $D_s(1^3D_3)$  and  $D_{s1}(2710)$ 's partner assignments for the  $D_{sJ}(2860)$  are likely; and (5) both the  $D_{s1}(2P)$  and  $D'_{s1}(2P)$  interpretations for the  $D_{sJ}(3040)$  seem possible. Further experimental studies on these states are needed.

## Acknowledgments

We acknowledge Prof. Xiang Liu for very helpful suggestions and discussions. This work is supported in part by HANCET under Contract No. 2006HANCET-02, and by the Program for Youthful Teachers in University of Henan Province.

## References

- [1] B. Aubert et al.(Babar Collaboration), Phys. Rev. D **80**,092003 (2009).
- [2] P. del Amo Sanchez et al. (BaBar Collaboration), arXiv:1009.2076 [hep-ex].
- [3] F. E. Close, C. E. Thomas, O. Lakhina, and E. S. Swanson, Phys. Lett. B **647**,159 (2006).



- [4] T. Matsuki, T. Morii, and K. Sudoh, Eur. Phys. J. A **31**, 701 (2007).
- [5] D. M. Li, B. Ma, and Y. H. Liu, Eur. Phys. J. C **51**, 359 (2007).
- [6] B. Chen, D. X. Wang, and A. Zhang, Phys. Rev. D **80**, 071502(R) (2009).
- [7] B. Zhang, X. Liu, W.Z. Deng, and S.L. Shu, Eur. Phys. J. C **50**, 617 (2007);  
W. Wei, X. Liu, and S. L. Zhu, Phys. Rev. D **75**, 014013 (2007).
- [8] E. vanBeveren and G. Rupp, Phys. Rev. Lett. **97**, 202001 (2006);  
E. VanBeveren and G. Rupp, Phys. Rev. D **81**, 118101 (2010).
- [9] P. Colangelo, F. DeFazio, and S. Nicotri, Phys. Lett. B **642**, 48 (2006) ;  
P. Colangelo, F. DeFazio, S. Nicotri, and M. Rizzi, Phys. Rev. D **77**, 014012 (2008).
- [10] P. Colangelo, F. DeFazio, Phys. Rev. D **81**, 094001 (2010).
- [11] X. H. Zhong and Q. Zhao, Phys. Rev. D **78**, 014029 (2008).
- [12] Z. F. Sun and X. Liu, Phys. Rev. D **80**, 074037 (2009).
- [13] X. H. Zhong and Q. Zhao, Phys. Rev. D **81**, 014031 (2010).
- [14] D. M. Li and B. Ma, Phys. Rev. D **81**, 014021 (2010).
- [15] Z. F. Sun, J. S. Yu, X. Liu, and T. Matsuki, Phys. Rev. D **82**, 111501 (2010).
- [16] X. H. Zhong, Phys. Rev. D **82**, 114014 (2010).
- [17] Z. G. Wang, Phys. Rev. D **83**, 014009 (2011).
- [18] Z. G. Wang, Chin. Phys. C **32**, 797 (2008);  
J. Vijande, A. Valcarce, and F. Fernandez, Phys. Rev. D **79**, 037501 (2009).
- [19] O. Lakhina and E. S. Swanson, Phys. Lett. B **650**, 159 (2007).
- [20] S. Godfrey and N. Isgur, Phys. Rev. D **32**, 189 (1985).
- [21] W. Lucha and F. F. Schoberl, Int. J. Mod. Phys. C **10**, 607 (1999).
- [22] T. A. Lahde, C. J. Nyfalt, and D. O. Riska, Nucl. Phys. A **674**, 141 (2000).
- [23] J. Zeng, J. W. Van Orden, and W. Roberts, Phys. Rev. D **52**, 5229 (1995).
- [24] D. Ebert, R. N. Faustov, and V. O. Galkin, Eur. Phys. J. C **66**, 197 (2010).
- [25] M. Di Pierro and E. Eichten, Phys. Rev. D **64**, 114004 (2001).
- [26] C. Amsler et al. (Particle Data Group), Phys. Lett. B **667**, 1 (2008).

- [27] K. Abe et al.(Belle Collaboration), arXiv:hep-ex/0608031;  
J. Brodzicka et al.Belle Collaboration), Phys. Rev.Lett.**100**,092001 (2008).
- [28] A. Le Yaouanc, L. Oliver, O. Pene, and J-C. Raynal, Hadron transistons in the quark model  
( Gordon and Breach Science Publishers, New York, 1988).
- [29] W. Roberts and B. Silvestr-Brac, Few-Body Syst. **11**, 171 (1992).
- [30] H. G. Blundel, arXiv:hep-ph/9608473.
- [31] T. Barnes, F. E. Close, P. R. Page, and E. S. Swanson, Phys. Rev. D **55**, 4157 (1997);  
T. Barnes, N. Black, and P. R. Page, Phys. Rev. D **68**, 054014 (2003).
- [32] E. S. Ackleh, T. Barnes, and E. S. Swanson, Phys. Rev. D **54**, 6811 (1996).
- [33] R. Kokoski and N. Isgur, Phys. Rev. D **35**, 907 (1987).
- [34] P. Geiger and E. S. Swanson, Phys. Rev. D **50**, 6855 (1994).
- [35] H.G. Blundell and S. Godfrey, Phys. Rev. D **53**,3700 (1996).
- [36] D. M. Li and B. Ma, Phys. Rev. D **77**, 074004 (2008);  
D. M. Li and B. Ma, Phys. Rev. D **77**, 094021 (2008);  
D. M. Li and S. Zhou, Phys. Rev. D **78**, 054013 (2008);  
D. M. Li and E. Wang, Eur. Phys. J. C **63**, 297 (2009).
- [37] A. Le Yaouanc, L. Oliver, O. Pene, and J. C. Raynal, Phys. Lett. B **72**, 57 (1977).
- [38] F. E. Close and E. S. Swanson, Phys. Rev. D **72**, 094004 (2005).
- [39] J. Lu, X. L. Chen, W. Z. Deng , and S. L. Zhu, Phys. Rev. D **73**, 054012 (2006); Z. G. Luo,  
X. L. Chen, and X. Liu, Phys. Rev. D **79**, 074020 (2009).
- [40] J. Koponen, Phys. Rev. D **78**, 074509 (2008).
- [41] W. Kwong and J. L. Rosner, Phys. Rev. D **38**, 279 (1988);  
S. Godfrey, Phys. Rev. D **70**, 054017 (2004);  
S. Godfrey, Phys. Rev. D **72**, 054029 (2005);  
G. J. Ding, J. J. Zhu, and M. L. Yan ,Phys. Rev. D **77**, 014033 (2008).